Chemical Engineering Journal 159 (2010) 91–97

Contents lists available at ScienceDirect

Chemical Engineering Journal

journal homepage: www.elsevier.com/locate/cej

Effect of solution chemistry on flux decline during high concentration protein ultrafiltration through a hydrophilic membrane

Ying Pei Lim [1], Abdul Wahab Mohammad *

Scale-Up and Downstream Processing Research Group, Department of Chemical and Process Engineering, Faculty of Engineering and Built Environment, Universiti Kebangsaan Malaysia, 43600 UKM Bangi, Malaysia

ARTICLE INFO

Article history:
Received 18 November 2009
Received in revised form 18 February 2010
Accepted 20 February 2010

Keywords:
Ultrafiltration
pH
Ionic strength
Fouling
Blocking models
Gelatin

ABSTRACT

The potential use of ultrafiltration (UF) in food industry has been well established. However there have been very few in-depth studies in understanding the fouling phenomena during the UF of food proteins, especially the random-coil type. In this study, the influence of solution chemistry on the extent of fouling and the associate fouling mechanism during UF has been investigated using concentrated gelatin with a hydrophilic regenerated cellulose acetate membrane (30 kDa MWCO). It was found that there was insignificant fouling under static condition, but severe fouling was observed during the dynamic filtration. The maximum flux decline rate was obtained at the isoelectric point (IEP) of gelatin, suggesting complementary electrostatically driven fouling. Addition of salt increased flux at pH values near the IEP but had a negative effect at pH above or below the IEP. The experimental data showed that both protein–protein and protein–membrane interactions influenced the gelatin ultrafiltration performance. The experimental data were fitted well into the fouling models thereby demonstrating that the solution chemistry influenced the fouling mechanism in gelatin ultrafiltration.

1. Introduction

Ultrafiltration (UF) is a pressure driven separation process, with membranes having pore sizes ranging from 1 to 100 nm. It is currently applied for the concentration of a wide range of protein products, including recombinant therapeutics, nutraceuticals, industrial enzymes, diagnostic products and a variety of food and beverages product [1,2]. However, membrane fouling by irreversible adsorption and/or deposition of solutes on and/or within the membrane, is the major drawback in membrane separation processes. In view of the fact that flux decline can severely affect the throughput and commercial feasibility of a manufacturing process, it is crucial to develop techniques to improve flux by understanding the cause of flux decline and elucidating the mechanism of fouling.

In general, the rate and extent of membrane fouling in protein ultrafiltration is affected by four factors, namely, membrane material, solution conditions, operating conditions and protein properties [3–8]. Particularly, electrokinetic effects such as membrane and solute charge, pH, ionic strength, have been shown to greatly influence the membrane fouling, water flux and solute retention [9–11]. Conversely, special structures and properties of different types of proteins can make separation process a complicated task. Proteins tend to interact with other components in the feed solution as well as adsorb onto polymeric membrane by the interaction mechanisms such as ionic, entropic, Van der Waals interactions and hydrogen bonding [12]. In most of protein ultrafiltration studies, fouling and adsorption have been found to be strongly dependent on protein–protein and protein–membrane interactions [13]. Protein–protein interactions affect the porosity of the cake layer on the membrane, while protein–membrane interactions affect irreversible adsorption onto the membrane [14]. Both interactions are usually affected by the pH and ionic strength of the feed solution. In fact, protein adsorption is maximum at pH values near the protein isoelectric point (IEP) under static and dynamic filtration mode [13,14]. At higher pH, where the protein and membrane (for negatively charged membranes) are of same sign, electrostatic repulsion created by the charged molecules and charged surface result in less fouling. Similar observations were reported by several researchers [15–17] that the protein rejection was highest under conditions where the membrane and protein had like charge due to strong electrostatic repulsion. At pH away from protein's IEP, as higher ionic strength solutions screen the charges in the system. This shielding effect reduces the hydrodynamic diameter of a protein, and also naturally decreases the charge of the membrane, which in turn increases the adsorption at membrane surface [18]. However, when proteins are at their IEP,

* Corresponding author. Tel.: +60 3 8921 4529; fax: +60 3 8921 4660.
E-mail address: wahabm@vlsi.eng.ukm.my (A.W. Mohammad).
[1] On study leave from Faculty of Chemical Engineering, Universiti Teknologi MARA, 40450 Shah Alam, Selangor, Malaysia.

1385-8947/$ – see front matter © 2010 Elsevier B.V. All rights reserved.
doi:10.1016/j.cej.2010.02.044

Nomenclature

A	available membrane frontal area (m^2)
J	flux (m/s)
J_o	initial pure water flux (m/s)
J_{wa}	pure water flux after experiment without permeate flux (static mode)
J_{ww}	pure water flux after dynamic filtration experiment
K_b	complete blocking constant (s^{-1})
K_c	cake filtration constant (s/m^2)
K_i	intermediate blocking constant (m^{-1})
K_s	standard blocking constant (m^{-1})
$MWCO$	molecular weight cut-off
V	permeate volume (L)
t	filtration time (s)
ΔP	transmembrane pressure (Pa)
R_{ad}	adsorption resistance (m^{-1})
R_f	fouling resistance (m^{-1})
R_m	membrane intrinsic resistance (m^{-1})
R_t	total filtration resistance (m^{-1})
μ	viscosity of permeate (Pa s)
ζ	streaming potential (mV)

normally the opposite effect is seen. These effects have been shown by Fane et al. [13,19].

For food proteins such as gelatin, a number of studies [20–23] have shown that ultrafiltration (UF) is feasible to concentrate mammalian and fish gelatin solution which contains 4–10% solids in water. However, limited study has been conducted on fouling characteristics and mechanism of gelatin ultrafiltration through manipulation of solution chemistry. Therefore, the objective of this paper is thus to obtain better understanding of the extent of adsorptive and dynamic fouling behavior in ultrafiltration of gelatin solution through the analysis of protein–protein and protein–membrane interactions. For this study, a hydrophilic type membrane, regenerated cellulose acetate, with 30 kDa MWCO was employed with a dead-end UF filtration mode. Typical fouling model centered on pore blocking is used to examine the effects of solution chemistry on fouling mechanisms in gelatin ultrafiltration.

2. Theory

Usually, flux decline behavior under constant pressure filtration can be analyzed in terms of four classic blocking laws, namely: standard blocking model, intermediate blocking model, cake filtration model and complete blocking model [24]. In a standard model, membranes have straight cylindrical pores that decline in effective radii as solid matter adsorb into the pore walls. When a portion of the membrane pores are unavailable for flow due to blockage of the pore, or solute attach to non-porous surfaces, the membrane is fouled by the complete or intermediate blocking mechanism. In the cake filtration model, the resistance to flow is increased by the presence of a cake layer on the membrane surface. The modes are illustrated in Fig. 1. The permeate volume for the all four models, as adapted from Bolton et al. [25] can be calculated as a function of time as shown in Table 1. In this study, the equations shown in Table 1 will be used to analyze the flux decline curves and identified the types of membrane fouling mechanisms at varying pHs and ionic strength.

Table 1
Summary of the typical blocking model as a function of time.

Model	Equation	Fitted parameter
Standard	$V = \left(\frac{1}{J_o t} + \frac{K_s}{2}\right)^{-1}$	K_s (m^{-1})
Intermediate	$V = \frac{1}{K_i} \ln(1 + K_i J_o t)$	K_i (m^{-1})
Complete	$V = \frac{J_o}{K_o}(1 - \exp(K_b t))$	K_b (s^{-1})
Cake	$V = \frac{1}{K_c J_o}\left(\sqrt{1 + 2K_c J_o^2 t} - 1\right)$	K_c (s/m^2)

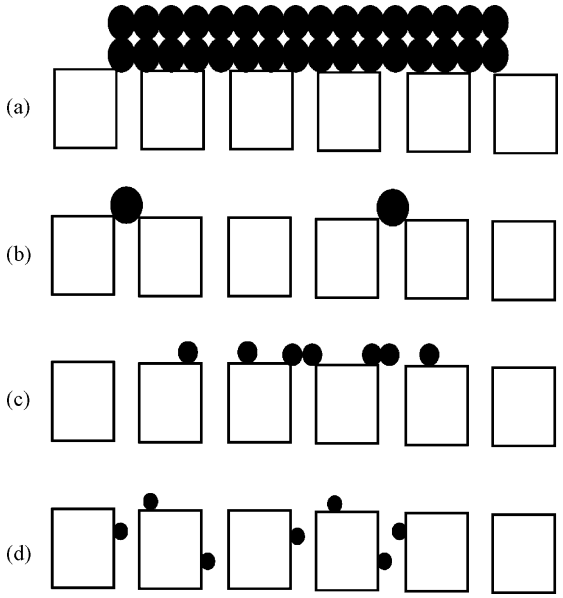

Fig. 1. Schematic diagram of membrane fouling mechanism: (a) cake formation, (b) complete pore blocking, (c) intermediate pore blocking and (d) standard blocking.

3. Materials and methods

3.1. Reagents

Hydrochloric acid from System ChemAR® and sodium hydroxide from R&M Chemicals, Essex, United Kingdom were used. Appropriate amount of sodium chloride (NaCl) were dissolved into the feed solution to control the ionic strength of the solution. The pH of solutions was measured with InoLab pH/Cond Level 1 meter (Weilheim, Germany) and pH of the medium was adjusted by adding either HCl or NaOH solutions. All reagents used in the experiments were of analytical grade unless otherwise stated. Water purified with Heal Force® Ultrapure Water System NW UF Series from Nison Instrument (Shanghai) Limited with resistivity of 18 MΩ cm was used for all experiments.

3.2. Characterization of model protein

In this study, industrial gelatin obtained from Halagel (M) Sdn. Bhd. was used as model protein without further purification. The structure gelatin is postulated to be a random coil with an electric charge which stems from the ionization of carboxyl or amino groups, resulting in repulsion and in expansion of the coil with varying pHs. The type-B gelatin was analyzed for pH, gel bloom strength, molecular weight distribution, viscosity and isoelectric point. A 6.67% (w/w) gelatin solution in ultrapure water (UPW) was prepared by mixing 7.5 g of the extracted gelatin and 105 mL of UPW. The mixture was left at room temperature for an hour to allow gelatin to swell. The mixture was later heated in a 65 °C bath for 20 min, stirring occasionally to assure that the gelatin is completely dissolved. The pH of gelatin was determined according to the BSI 757:1975 standard test method [26] using inoLab pH/Cond Level 1 pH meter at 60 °C. Gel strength was determined according to GME Monograph Standardised Methods for the Testing of Edible Gelatin

Table 2
Characteristic of UF membrane used.

Membrane	30 kDa Ultracel®
Filter material[a]	Regenerated cellulose acetate
Surface charge[b]	Neutral [28]
pH tolerance[a]	2–13
Hydrophobicity[a]	Hydrophilic
Contact angle (°)[c]	12 ± 2.94
Average pore size (nm)[b]	6.1 [29]
Isoelectric point[b]	~3.5 [30]
Hydraulic permeability (lmh bar)[c]	305.67 ± 16.67

[a] Information obtained from manufacturer.
[b] Adapted from the literature.
[c] Value obtained from experimental measurements in triplicate.

by using TA.HDPlus texture analyzer (Stable MicroSystems, UK). The load cell and the speed of the plunger (ϕ = 12.7 mm) were 5 kN and 0.5 mm/s, respectively, with the penetration depth of 4 mm was recorded. Viscosity was determined with a Brookfield DV II+ Pro viscometer (Middleboro MA, USA) equipped with a No. 1 spindle at 100 rpm by starting at 60 °C and then reducing temperature at a rate of 0.5 °C/min till solution gelling. The measurements were carried out in triplicate. Molecular weight distribution was determined using chip-based separations performed on the Agilent 2100 Bioanalyzer (Santa Clara, USA) in combination with the Agilent High Sensitivity Protein 250 Kit and the dedicated 2100 Expert software assay. The chip was prepared according to the protocol provided with the High Sensitivity Protein 250 kit [27]. As for the determination of isoelectric point (IEP), gelatin solutions (0.1%, w/w) were titrated with 0.25 M NaOH and 0.25 M HCl and the zeta potential at a given pH were recorded by a zeta potential titration apparatus using Malvern Zetasizer Nano ZS, UK. The isoelectric points of the samples were determined at the pH value where the zeta potential was zero.

3.3. Membrane characterization and experimental set-up

Ultrafiltration (UF) disc membrane made of asymmetric regenerated cellulose acetate (PLTK Ultracel®), obtained from Millipore, were used in the static and dynamic ultrafiltration experiments. The nominal molecular weight cut-off (MWCO) of the membranes as reported by the manufacturer was 30,000 Da. All disc membranes had a diameter of 76 mm with a geometric (flat surface) area of 28.7 cm^2. Characteristic of the membrane is shown in Table 2. A dead-end stirred cell filtration system was used to characterize the static and dynamic filtration performance as shown in Fig. 2. All ultrafiltration experiments were carried out using a filtration test cell (Model 8200, Millipore Co., USA) with volume capacity of 200 mL. The stirred cell was connected to an acrylic solution reservoir of 800 mL via a selector. The

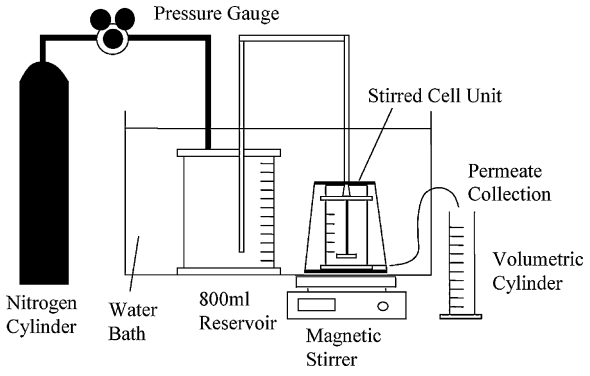

Fig. 2. Schematic diagram of dead-end stirred cell for gelatin ultrafiltration.

operation pressure in the system was maintained by nitrogen gas.

3.4. Fouling experiments

Gelatin with concentration of 4% (w/w) at various pH values and ionic strength was used as feed solution. Each membrane experiments were carried out with a new membrane disc. To prevent any compaction effects, each membrane was initially compacted with ultrapure water for 30 min at 2.5 bar. Then the clean membrane hydraulic permeability (L_{po}) was calculated for each membrane sample from the slope of data for the filtrate flux (J) as a function of applied pressure ΔP between 0.5 and 2 bar. For static adsorption test, the cell was filled with gelatin solution with stirring effect for 24 h without any applied pressure. Thereafter, the solution was removed, and the membrane surface was rinsed two times by filling the cell with pure water (100 mL) and shaking it for 30 s. Pure water flux was measured again and membrane permeability after adsorption (L_{pa}) was recalculated afterwards. The evaluation of membrane performance was done by calculating the relative permeability reduction according to:

$$RPR\ (\%) = \frac{L_{po} - L_{pa}}{L_{po}} \times 100\% \quad (1)$$

with RPR being the relative permeability reduction. L_{po} and L_{pa} are permeability before and after adsorptive, respectively.

In the case of dynamic ultrafiltration test, the feed solution was conducted under constant pressure at 2 bar. The suspended bar impeller inside the stirred cell was magnetically driven by a stirrer (WiseStir, USA). The highest speed of 500 rpm was selected because it could provide effective agitation but prevent the formation of a series vortex in the cell. Care was also taken to avoid entrapment of air bubbles in the flow path or within the filter holder. Permeate flux was calculated based on the mass of permeate collected on the balance. After 60 min, the filtration was stopped and the cell and the solution reservoir were fully emptied and gently rinsed to remove any labile protein. Rinsing was done by filling the stirred cell with ultrapure water twice and shaking it for 30 s in the absence of any applied transmembrane pressure. The cell was then filled with ultrapure water and re-pressurized, and the pure water flux was evaluated to quantify fouling. Fouling can be quantified by the resistance appearing during the filtration. The resistance is due to the formation of foulants layer on the membrane surface. The flux (J), through the foulants layer and the membrane, is given by:

$$J = \frac{\Delta P}{\mu \sum R} \quad (2)$$

where ΔP is the transmembrane pressure (driving force), μ is the viscosity of permeate and $\sum R$ or (R_t) is the sum of the resistances ($R_t = R_m + R_{ad} + R_f$). The intrinsic membrane resistance (R_m) which is characterized by mainly the pore shape and size and membrane thickness, as determined during the manufacturing process can be estimated from the initial pure water flux, J_o:

$$R_m = \frac{\Delta P}{\mu J_o} \quad (3)$$

R_{ad} is defined as a filtration resistance caused by adsorption of foulants on membrane surface which can be calculated from equation below:

$$R_{ad} = \left(\frac{\Delta P}{\mu J_{wa}}\right) - R_m \quad (4)$$

Fouling resistance caused by irreversible and reversible adsorption of foulants on membrane pore wall or surface (R_f) can be calculated

Table 3
Principle characteristics of the gelatin solution.

Properties	Value
Gel bloom	246 ± 0.39
pH at 40 °C	5.3 ± 0.01
MW range (kDa)	10–420
Mean MW (kDa)	195 ± 0.53
Gelling temperature (°C)	32.8 ± 0.01
Viscosity (cP)	7.02
Isoelectric point (IEP)	5.04

as follows:

$$R_f = \left(\frac{\Delta P}{\mu J_{ww}}\right) - R_m - R_{ad} \quad (5)$$

4. Results and discussion

4.1. Gelatin characterization

In designing ultrafiltration process, it is important that the emphasis is on studying all the parameters affecting the membrane performance and achieving the desired level of separation for the application of interest. In protein ultrafiltration, one of the crucial parameters is the protein properties which affect the permeability and the retention of the membrane process. Table 3 shows the main physicochemical properties of gelatin solution used in the experiment. Since the molecular weight range, obtained through SDS-PAGE is within 10–420 kDa, ultrafiltration membrane with MWCO of 30 kDa was used in the static and dynamic filtration experiment. Three different pHs were selected to examine the effect of pH on the fouling behavior of gelatin ultrafiltration, i.e., pH solution near IEP of gelatin (pH 5.3) and pH solution above and below gelatin IEP (pH 4 and pH 6.8). All experiments were carried out at a temperature of 40 ± 2 °C, above the gelling point of gelatin.

4.2. Static adsorption

For RCA UF membrane, no variation in RPR was observed for the first 4 h (result no shown), and subsequently, 24 h exposure time was chosen for the adsorptive fouling test. It seemed that minimum adsorption of gelatin occurred in static condition. The permeability of the RCA UF membranes was not significantly affected by adsorption of gelatin. This is proven by the fact that the permeability after protein adsorption was always within 10% of the clean membrane permeability. This phenomenon is usually observed for membrane material with low protein binding capacity, such as cellulose acetate type. This might be due to the membrane material which is totally ionic and contains no apolar regions to bind protein by hydrophobic interaction. Beside the drop in permeability, the adsorption resistance, which is a measure of the extent of adsorption, can be determined using equation (4). In comparing the contribution of adsorption fouling by resistance model, R_{ad}/R_m was calculated as 0.956 ± 0.00454, not in agreement with the findings obtained by Ognier et al. [31]. They found that the adsorption resistance was relatively small compared to actual fouling resistance and that R_{ad}/R_m was roughly 0.33 after contacting with the protein solution of 5 g/l without permeate flux. Adsorption resistance obtained in this study was rather high due to high gelatin concentration used, which was 42 g/l.

4.3. Dynamic adsorption

4.3.1. Effect of pH

To investigate membrane–solute–solute interactions, dead-end stirred ultrafiltration was performed with constant transmembrane pressure at 2 bar. The fouling behavior of gelatin using UF membrane for several pHs is shown in Fig. 3. The results are presented in terms of permeate flux relative to initial water flux (J/J_o) for easy comparison of the figures. The data clearly demonstrate that the permeate flux was quite responsive to the solution pH. Fane et al. [13,19] and Suki et al. [32] also demonstrated that the solution pH plays a significant role in the controlling the extent of fouling in protein ultrafiltration.

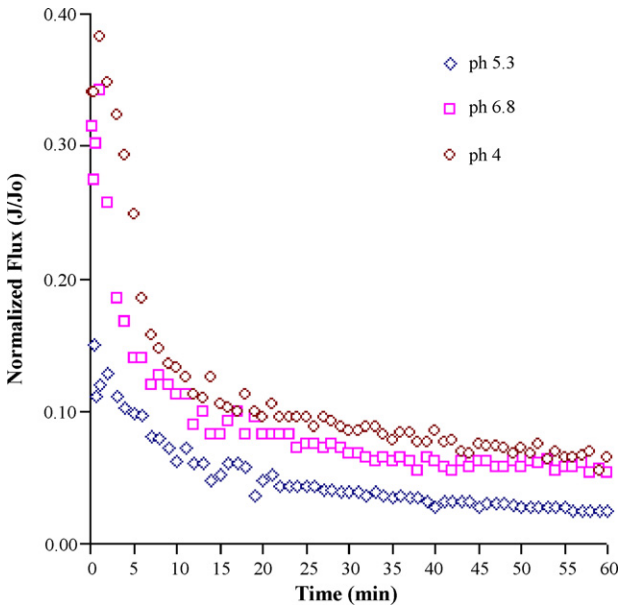

Fig. 3. Flux decline profile for several pHs through regenerated cellulose acetate membrane with gelatin solution at 4% (w/w).

Two different flux regimes can be clearly seen in Fig. 3: a rapid flux decline at the initial time of filtration followed by gradual flux declines for all the solution conditions. This decrease leads to final fluxes of about 5–10% of the initial flux, in a time span of 1 h. Previous investigators have observed similar patterns with retentive ultrafiltration membranes. Over the pH range examined, permeate flux measured was lowest at pH 5.3, which corresponded to the pH near IEP of gelatin. This observation could be reasonably explained by the protein–membrane interactions through the degree of electrostatic repulsion between gelatin and the RCA UF membrane. Since the IEP of RCA UF membrane is ~3.5, the membrane shall have negative charge on its surface for all the pH range employed in the experiment. On the other hand, the effect of pH on the net charge of proteins is summarized below. When the pH of a protein solution is lower than the isoelectric point (IEP) of the protein (i.e., pH < IEP), the protein molecules carry positive charges, as shown in Eq. (6). On the contrary, when the pH value of a protein solution is higher than the IEP value of the protein (i.e., pH > IEP), the dissociation of carboxyl groups is increased and the H_2N–$RCOO^-$ anions, i.e., the negative charges will predominate [33].

$$\begin{aligned} &R\text{–}NH_2 + H^+ \rightarrow R\text{–}NH_3{}^+ \\ &R\text{–}COO^- + H^+ \rightarrow R\text{–}COOH \end{aligned} \quad (6)$$

$$\begin{aligned} &R\text{–}NH_3{}^+ + OH^- \rightarrow R\text{–}NH_2 + H_2O \\ &R\text{–}COOH + OH^- \rightarrow R\text{–}COO^- + H_2O \end{aligned} \quad (7)$$

At pH 5.3, which was very near to the IEP, the gelatin molecule carries no net charge and the molecule is in its most compact state at that point. Consequently, electrostatic repulsion between gelatin and the UF membrane was weakest and gelatin could easily accumulate on the membrane surface relatively densely to form a compact configuration under convectional flux. As a result of this, the flow resistance increases distinctly at pH around the IEP. Experimental study has shown that the low filtration flux in dead-end

Table 4
Comparison of R_f/R_m and R_t/R_m for varying pHs.

pH	R_f/R_m	R_t/R_m
4	0.368	1.3684
5.3	1.058	2.0576
6.8	0.424	1.4238

ultrafiltration around the IEP is due mainly to the build-up of compact filter cake [34,35]. For pH away from gelatin's IEP, the stronger electrostatic repulsion between gelatin and the UF membrane led to much lesser accumulation of gelatin on membrane surface. At pH 4, apart from the electrostatic repulsion between gelatin and the gelatin-adsorbed membrane surface, the electrostatic attraction between gelatin (positively charged) and the fresh membrane (negatively charged) affected the flux decline. Above the IEP of the protein, i.e., at pH 6.8, the surface of RCA UF as well as the protein had negative charges resulting electrostatic repulsion created by protein–membrane interactions, thus less of this larger gelatin can fit on the membrane surface [14].

It should be noted that the fluxes after 60 min were significantly different for different solution conditions with the same membrane, indicating the significant contribution of fouling towards the flux reduction. An attempt was made to relate the total filtration resistance and fouling resistance for different pHs, as shown in Table 4. The total resistance and fouling resistance were maximum at pH 5.3, minimum at pH 4 and intermediate at pH 6.8. This observation is in agreement with the flux decline profile reported in Fig. 2. Nevertheless, higher permeate flux observed at pH 4 as compared to pH 6.8 is quite surprising and contradict the previous work [13,19] studying protein fouling in ultrafiltration. Clearly, in this case, both protein–membrane interactions and protein–protein interactions are responsible for the trend depicted in Fig. 3. One plausible reason could be the inevitable adsorption of gelatin may modify the nature of the membrane surface, i.e., formed-in-place secondary layer membrane that controls original membrane behavior [36–38]. It might be that the charge on the protein, rather than the difference in charge between the membrane and the protein, determines the extent of hydraulic resistance and flux at varying pHs. Another possible explanation could arise from the reduction in molecular size and lower zeta potential of gelatin solution at pH 4 compared to that at pH 6.8 as shown in Table 5. The more compact molecular configuration of gelatin and electrostatic attraction of RCA UF membrane and gelatin molecules at pH 4 can contribute to the formation of a denser fouling layer with flat conformation, but it would also allow some gelatins to more readily penetrate through membrane pores. Protein fouling potential may thus be decreased due to less amount of gelatin retained by the RCA UF membranes, resulting in thinner layer of foulants.

4.3.2. *Effect of ionic strength*

To investigate the effect of ionic strength on gelatin fouling potential, UF experiments were conducted by addition of sodium chloride (NaCl) to a concentration of 0.1 M. The resultant flux profile compared to without the presence of salt at varying pHs is shown in Fig. 4. It was found that the ionic strength of the solution also

Table 5
Gelatin charge, membrane surface charge and gelatin hydrodynamic radius at pH 4 and pH 6.8.

pH	Protein ζ (mV) at 0.1% (w/v) [39]	Membrane ζ (mV) [30]	Hydrodynamic radius (nm) [40]
4	+3	−5.4	~22
6.8	−20	−20.0	~18.4[a] at pH 6.62

[a] Gelatin-B aqueous solution at 25 °C, with concentration about 0.5 kg/m^3.

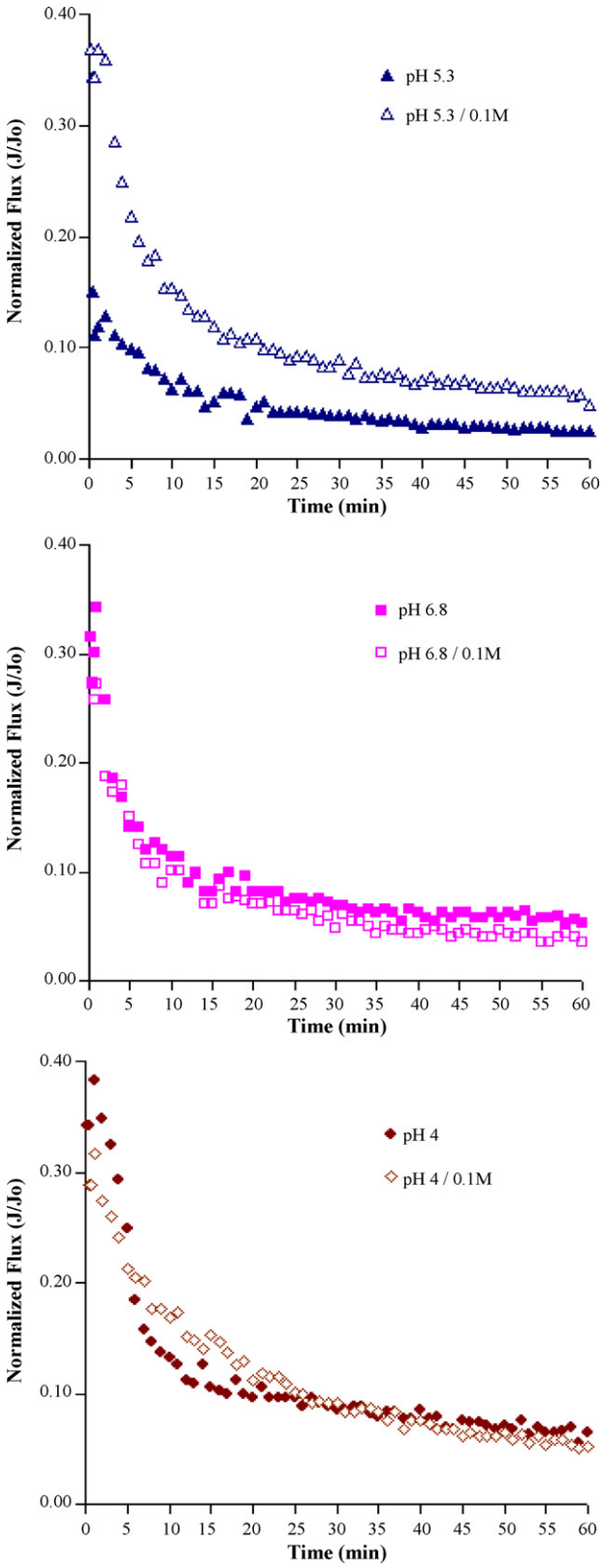

Fig. 4. Flux decline during the constant pressure filtration of 4% (w/w) gelatin solutions at 2 bar and various pHs, with and without salt.

Table 6
Comparison of R_f/R_m and R_t/R_m for varying pHs and ionic strength 0.1 M.

pH	R_f/R_m	R_t/R_m
4/0.1 M	0.321	1.321
5.3/0.1 M	0.186	1.186
6.8/0.1 M	0.366	1.366

affected the extent of fouling. With increased of ionic strength in the gelatin solution, it will result in lower flux at pH away from gelatin's IEP, i.e., pH 4 and pH 6.8, but greater flux improvement at pH near the gelatin's IEP. Total filtration resistance and fouling resistance for different pHs with added salt, as shown in Table 6 are in agreement with the flux decline curve reported in Fig. 4. With salt added, the gelatin solution away from the gelatin's IEP resulted in higher fouling than gelatin solution having pH near the protein IEP as noticed by the increase in fouling resistance.

Addition of salt which suppresses the binding at pH away from gelatin's IEP can be elucidated by the charge-screening effect and double layer compression [41–43]. With the increase in counterions with ionic strength, the shielding effect will be enhanced and thus the gelatin molecules act more like uncharged molecules. This would reduce electrostatic repulsion between the gelatin-adsorbed membrane and gelatin, or between gelatin molecules. As a result, more gelatins would have an easier approach towards the membrane surface and thus expedited the accumulation of gelatin on the membrane surface, which contributed to the formation of a thicker fouling layer. Moreover, at constant gelatin concentration, the hydrodynamic radius was found to decrease with increasing solution ionic strength due to charge shielding and consequently form a more compact fouling layer. Therefore, higher flux decline, is expected with increasing ionic strength. On the other hand, at pH near to the IEP of gelatin, the functional groups with opposite charges within the gelatin molecule attracted one another to form a compact molecular structure with zero net charge. When salt was added, this manifests the effect of charged surface due to anion binding, enlargement of the molecule and acquisition of charge. As a result, a slightly larger molecule formed a more porous fouling layer and higher fluxes are observed. However, no obvious reduction in initial flux at pH away from gelatin's IEP as seen in Fig. 4 is interesting. This trend could be due to a smaller Debye length at the high salt concentrations which causes faster reduction in the magnitude of the electro-osmotic counterflow. Lower flux at the steady state might be due to the reduced intermolecular electrostatic repulsion at the higher salt concentration.

4.3.3. Fouling mechanism

In order to reveal how the fouling mechanism depends on solution chemistry, the permeate volume versus time data was fitted using the typical fouling models as shown in Table 1 (cf. Section 2) using Matlab R2007a. The best fit parameter was obtained by minimizing the sum of squared residuals (SSR) where the residual was equal to the difference between any experimental data point and the corresponding model prediction. An example of the fitting of experimental data and model prediction is shown in Fig. 5 for dynamic filtration at pH 6.8. As depicted from the figures, the best fit data for dynamic filtration at pH 6.8 occurred with the cake model, which had the minimum SSR compared to other fouling models. The rest of the fitted parameter and SSR for other solution chemistry is shown in Table 7.

Table 7
Best fitted model for different solution chemistries used in the experiment.

Solution chemistry	Best fitted model	Fitted parameter values
pH 4	Intermediate	$K_i = 28.22\ m^{-1}$
pH 4/0.1 M	Intermediate	$K_i = 25.32\ m^{-1}$
pH 5.3	Standard	$K_s = 25.09\ m^{-1}$
pH 5.3/0.1 M	Intermediate	$K_i = 28.50\ m^{-1}$
pH 6.8	Cake	$K_c = 1.82 \times 10^6\ s/m^2$
pH 6.8/0.1 M	Cake	$K_c = 3.10 \times 10^6\ s/m^2$

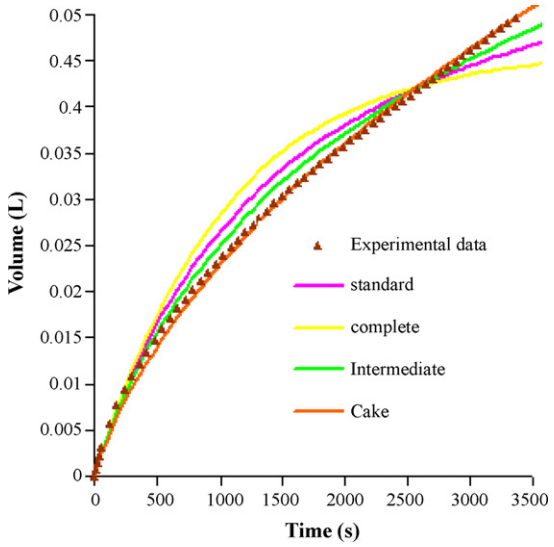

Fig. 5. Permeate volume vs time data compared standard model, complete model, intermediate model and cake model for 4% (w/w) gelatin solution at 2 bar and pH 6.8.

Generally, it was found that the fouling mechanism is affected by the change in solution pH and the sign of protein charge. For the range of pH studied here, the protein charges changed from positive (pH 4) to negative (pH 6.8) passing through neutral at IEP (pH 5.04). It is postulated that fouling mechanism changes from internal blocking to external fouling in response to protein net charge, and thus it is mainly controlled by electrostatic interactions forces for hydrophilic type ultrafiltration membrane. However, it was found that the fouling mechanism dominating the flux decline did not change significantly at pH away from protein IEP, with or without the presence of salt, possibly due to the insignificant of charge-screening effect on positively/or negatively charged gelatin. Although the mechanism of fouling and the initiation and growth of protein deposits has been studied in some detail [44], but the conditions leading up to fouling, especially in the presence of salts and varying pH values, are not well understood.

5. Conclusion

It has been shown that solution pH and ionic strength have significant effect on the extent of protein fouling in membrane processes. With regard to the permeate flux, the maximum flux decline occurred at pH 5.3, i.e., around the isoelectric point of gelatin. This could be due to the development of membrane fouling caused by the formation of dense and compact foulant layer at membrane surface. On the other hand, increasing fluxes were observed at pH away from IEP (pH 4 and pH 6.8) since protein–protein and membrane–protein repulsions avoid aggregation and fouling. The presence of electrolytes in feed solutions reduced fouling with a consequent increase in the flux at pH values at the IEP but had a negative effect at pH above or below the IEP. It was observed that the fluxes showed the behavior expected from the conformational changes and charge effects which then lead to variations in the permeability of the protein that match the variations of flux with pH and salt content. However, the real mechanism of the ultrafiltration of the protein solutions was quite complicated. It is postulated that fouling mechanism changed from

internal blocking to external fouling in response to protein charge state.

Acknowledgements

The authors would like to acknowledge the financial grant funded by Universiti Kebangsaan Malaysia via grant UKM-GUP-KPB-08-32-129 and TF0206A084. The authors would also like to acknowledge Halagel (M) Sdn. Bhd. for donation of the gelatin.

References

[1] T.Y. Wu, A.W. Mohammad, J.Md. Jahim, N. Anuar, Palm oil mill effluent (POME) treatment and bioresources recovery using ultrafiltration membrane: effect of pressure on membrane fouling, Biochem. Eng. J. 35 (3) (2007) 309–317.
[2] W.K. Wang, Membrane Separations in Biotechnology, 2nd ed., Marcel Dekker Inc., 2001.
[3] J. Cho, G. Amy, J. Pellegrino, Membrane filtration of natural organic matter: initial comparison of rejection and flux decline characteristics with ultrafiltration and nanofiltration membranes, Water Res. 33 (1) (1999) 2517–2526.
[4] G.F. Crozes, J.G. Jacangelo, C. Anselme, J.M. Laîné, Impact of ultrafiltration operating conditions on membrane irreversible fouling, J. Membr. Sci. 124 (1997) 63–76.
[5] C. Herrero, P. Prádanos, J.I. Calvo, F. Tejerina, A. Hernández, Flux decline in protein microfiltration: influence of operative parameters, J. Colloid Interface Sci. 187 (1997) 344–351.
[6] C. Güell, R. Davis, Membrane fouling during microfiltration of protein mixtures, J. Membr. Sci. 119 (1996) 269–284.
[7] M.K. Ko, J.J. Pellegrino, R. Nassimbene, P. Marko, Characterization of the adsorption-fouling layer using globular proteins on ultrafiltration membranes, J. Membr. Sci. 76 (1993) 101–120.
[8] E. Matthiasson, The role of macromolecular adsorption in fouling of ultrafiltration membranes, J. Membr. Sci. 16 (1983) 23–36.
[9] Y. Mukai, E. Iritani, T. Murase, Effect of protein charge on cake properties in dead-end ultrafiltration of protein solutions, J. Membr. Sci. 137 (1997) 271–275.
[10] K. Ohmori, C. Glatz, Effects of pH and ionic strength on microfiltration of *C. glutamicom*, J. Membr. Sci. 153 (1999) 23–32.
[11] L. Ricq, S. Narcon, J.-C. Reggiani, J. Pagetti, Streaming potential and protein transmission ultrafiltration of single proteins in mixture: β-lactoglobulin and lysozyme, J. Membr. Sci. 156 (1999) 81–96.
[12] C.H. Müller, G.P. Agarwal, Th. Melin, Th. Wintgens, Study of ultrafiltration of a single and binary protein solution in a thin spiral channel module, J. Membr. Sci. 227 (2003) 51–69.
[13] A.G. Fane, C.J.D. Fell, A. Suki, The effect of pH and ionic environment on the ultrafiltration of protein solutions with retentive membranes, J. Membr. Sci. 16 (1983) 195–210.
[14] K. Jones, C. O'Melia, Protein and humic acid adsorption onto hydrophilic membrane surfaces: effects of pH and ionic strength, J. Membr. Sci. 165 (2000) 31–46.
[15] D.B. Burns, A.L. Zydney, Contribution to electrostatic interactions on protein transport in membrane systems, AIChE J. 47 (2001) 1101–1113.
[16] S. Nakao, H. Osada, H. Kurata, T. Suru, S. Kimura, Separation of proteins by charged ultrafiltration membranes, Desalination 70 (1998) 191–202.
[17] R.V. Reis, J.M. Brake, J. Charkoudian, D.B. Burns, A.L. Zydney, High performance tangential flow filtration using charged membranes, J. Membr. Sci. 159 (1999) 133–142.
[18] L. Palacio, J.I. Calvo, P. Prádanos, A. Hernández, P. Väisänen, M. Nyström, Contact angles and external protein adsorption onto UF membranes, J. Membr. Sci. 152 (1999) 189–201.
[19] A.G. Fane, C.J.D. Fell, A.G. Waters, Ultrafiltration of protein solutions through partially permeable membranes: the effect of adsorption and solution environment, J. Membr. Sci. 16 (1983) 211–224.
[20] A. Simon, L. Vandanjon, G. Levesque, P. Bourseau, Concentration and desalination of fish gelatin by ultrafiltration and continuous diafiltration process, Desalination 144 (2002) 313–318.
[21] B. Dutré, G. Trägårdh, Purification of gelatin with a forced solvent stream along the membrane permeate side: an experimental approach, J. Food Eng. 25 (1995) 233–244.
[22] B. Chakravorty, D.P. Singh, Concentration and purification of gelatin liquor by ultrafiltration, Desalination 78 (1990) 279–286.
[23] R. Skelton, Membrane technology: technical and applications brief, Paper Presented at a Meeting of the Society of Chemical Industry, London, 1986.
[24] J. Hermia, Constant pressure blocking laws—application to power law non-Newtonian fluids, Trans. IChemE 60 (1982) 183–187.
[25] G. Bolton, D. LaCasse, R. Kuriyel, Combined models of membrane fouling: development and application to microfiltration and ultrafiltration of biological fluids, J. Membr. Sci. 277 (1–2) (2006) 75–84.
[26] BSI (British Standards Institution), Methods for Sampling and Testing Gelatin (Physical and Chemical Methods), 1975, London.
[27] Agilent Technologies, Inc., Agilent high sensitivity protein 250 kit guide. Available at: www.agilent.com/chem/labonachip, 2008 (accessed 31.03.09).
[28] B. Kwon, J. Molek, A.L. Zydney, Ultrafiltration of PEGylated proteins: fouling and concentration polarization effects, J. Membr. Sci. 319 (1–2) (2008) 206–213.
[29] J.-D. Jeon, S.J. Kim, S.-Y. Kwak, H nuclear magnetic resonance (NMR) cryoporometry as a tool to determine the pore size distribution of ultrafiltration membranes, J. Membr. Sci 309 (2008) 233–238.
[30] R. Chan, V. Chen, M.P. Bucknall, Ultrafiltration of protein mixtures: measurement of apparent critical flux, rejection performance, and identification of protein deposition, Desalination 146 (1–3) (2002) 83–90.
[31] S. Ognier, C. Wisniewski, A. Grasmick, Influence of macromolecule adsorption during filtration of a membrane bioreactor mixed liquor suspension, J. Membr. Sci. 209 (2002) 27–37.
[32] A. Suki, A.G. Fane, C.J.D. Fell, Flux decline in protein ultrafiltration, J. Membr. Sci. 21 (1984) 269–283.
[33] R. Westermerier, V.C.H. Weinheim, Electrophoresis in Practice, 1993, New York.
[34] E. Iritani, S. Nakatsuka, H. Aoki, T. Murase, Effect of solution environment on unstirred dead-end ultrafiltration characteristics of proteinaceous solution, J. Chem. Eng. Jpn. 24 (1991) 177–183.
[35] E. Iritani, T. Watanabe, T. Murase, Effects of pH and solvent density on dead-end upward ultrafiltration, J. Membr. Sci. 69 (1992) 87–97.
[36] N.K. Saha, M. Balakrishnan, M. Ulbricht, Polymeric membrane fouling in sugarcane juice ultrafiltration: role of juice polysaccharides, Desalination 189 (1–3) (2006) 59–70.
[37] J. Bullón, M.P. Belleville, G.M. Rios, Preparation of gelatin formed-in-place membranes: effect of working conditions and substrates, J. Membr. Sci. 168 (1–2) (2000) 159–165.
[38] P.V. Stevens, M. Nyström, N. Ehsani, Modification of ultrafiltration membrane with gelatin protein, Biotechnol. Bioeng. 57 (1) (1998) 26–34.
[39] B. Mohanty, A. Gupta, S. Bandopadhay, H.B. Bohidar, Effect of gelatin molecular charge heterogeneity of intermolecular complexes and coacervation transition, J. Polym. Sci. B: Polym. Phys. 45 (2007) 1511–1520.
[40] W. Lin, L. Yan, C. Mu, W. Li, M. Zhang, Q. Zhu, Effect of pH on gelatin self-association investigated by laser light scattering and atomic force microscopy, Polym. Int. 51 (2002) 233–238.
[41] S. Madaeni, S. Sedeh, M. De Nobili, Ultrafiltration of humic substances in the presence of protein and metal ions, Transport Porous Media 65 (3) (2006) 469–484.
[42] S. Salgn, S. Takac, T.H. Ozdamar, A parametric study on protein–membrane–ionic environment interactions for membrane fouling, Sep. Sci. Technol. 40 (6) (2005) 1191–1212.
[43] A. Persson, A.-S. Jönsson, G. Zacchi, Transmission of BSA during cross-flow microfiltration: influence of pH and salt concentration, J. Membr. Sci. 223 (1–2) (2003) 11–21.
[44] S.T. Kelly, A.L. Zydney, Mechanisms for BSA fouling during microfiltration, J. Membr. Sci. 107 (1995) 115–127.